Multiple Laser Beam Combining and Phasing Using Closed-Loop Control

D. R. Neal, T.G. Smith, G.R. Eisler, J.L. Wilcoxen, R.R. Rosenthal
Sandia National Laboratories, Albuquerque, New Mexico 87185

ABSTRACT

One method for scaling lasers to higher power is to build several separate amplifier chains, and then coherently combine the individual beams together. To combine the beams the pathlengths must be matched to an integer number of waves, and the tip and tilt of each beam must be the same. Since optical tolerances are fractional micrometers, a sophisticated control system must be employed to actively measure tip/tilt and piston errors, and apply real time corrections. We have developed a test bed that allows us to develop the required control algorithms for two to four beams and then scale to a larger numbers.

1. INTRODUCTION

The scaling of laser systems to high power presents many challenges. In general, it is important to preserve good beam quality while increasing the laser power. Controlling the beam quality is often the most difficult task in the scaling operation, and has resulted in limitations imposed on several large lasers[1]. For a system that can be scaled by increasing the number of laser beams, the laser extraction optics ultimately determine the beam quality of the device. For some systems it is difficult to use a single resonator and increase the length, width or height. Thus the gain region is broken up into several potentially uncoupled regions. Power is extracted through means of either a set of coupled resonators[2] or through a master oscillator/power amplifier (MOPA) arrangement. Both of these approaches have been used with reasonable success. In either case, the laser system produces more than a single beam, since each gain region is relatively independent. In some cases these beams are at the same frequency, but have different piston/tip and tilt, and in others the beams are multi-line or have different frequency content as well. The beam control system must combine these beams coherently to use them efficiently.

In order to combine beams from such a laser source, a phasing system is needed. This can take several forms. While some researchers have had success with a variety of non-linear optical techniques, we are investigating stitching together several beams side-by-side with a closed loop control system that is capable of measuring the phase or beam quality of the combined system. This offers some flexibility in the choice of the laser source and in the power of the beam. In addition, it is the only likely beam combining candidate for low power beams.

The discrete beam phasing technology is closely related to adaptive optics that are used for imaging of objects through turbulent media[3, 4, 5, 6, 7]. This technique has often been applied to astronomical[5, 6, 7] and solar[8, 9] imaging. For discrete beam combining, the segmented approach is preferable to the continuous facesheet adaptive optic, since each beamlet is assumed to have fairly good beam quality by itself.

For a single line laser system phasing must be accomplished only to the nearest integer wavelength. For a multi-line system, the pathlength must be matched absolutely throughout the entire optical train. While both of these systems require phase control to a fraction of wave, the phase sensing problem is simplified somewhat for a single line laser, since phase ambiguities across 2π are not important. This work is an attempt to evaluate the feasibility of a single-line phasing system, and to evaluate a variety of phase sensing concepts.

We have approached the multiple beam combining problem in several stages. The first was to evaluate a number of phasing methodologies and work out the required optics and other hardware, with the second being the development of several mirror modules. The final scaling will involve building a large mirror system using a number of these modular building blocks. In addition to the mirror/actuator systems, we are evaluating a variety of phase sensing technologies and a number of control algorithms. Throughout this work the scalability to a large number of mirrors has been carefully considered, and experiments have been defined to evaluate it.

2. WAVEFRONT SENSING TECHNIQUES

A number of phase sensing technologies and architectures are appropriate for the beam combining problem. These include Shack-Hartmann wavefront sensing, interferometry, shear plate interferometry, and far-field wavefront sensing. We have evaluated several of these and chosen a few for testing in the beam combining testbed.

0-8194-1153-1/93/$6.00

2.1 Shack-Hartmann wavefront sensing

A Shack-Hartmann wavefront sensor has a number of advantages for wavefront sensing in a beam combining application. It can produce accurate information about the tip/tilt errors of individual segments in the beam at high bandwidths. The Shack-Hartmann sensor is relatively simple in concept, consisting of only a lens array and a CCD camera in its simplest implementation. Shack-Hartmann sensors are in common use for beam control in other adaptive optic systems[8, 10, 11, 12, 13]. The hardware, algorithms and processing have been developed to a considerable extent, with even commercial systems beginning to appear[11].

One drawback of the Shack-Hartmann sensor is that it measures wavefront slope, not wavefront height. Thus an integration step must be performed in the processing in order to convert the wavefront slope to wavefront error information. This data interpretation is often time consuming or requires significant specialized hardware. For most imaging systems where a significant jump in phase from segment to segment is not expected, this provides all of the information necessary. By matching the edges of adjacent segments the wavefront is reconstructed without additional measurements[9, 13] Unfortunately, for a multi-segmented beam where the piston of one segment bears no relation to its neighbor, this technique cannot be used. The wavefront slope information can be used directly to control the pointing of the beams at fairly high bandwidth (~1–2 kHz have been demonstrated), and, since each segment is independent, there is no coupling of one beam to the next.

One concept for wavefront sensing is to use a Shack-Hartmann sensor for high speed tip and tilt measurements, and then compute the piston from a separate measurement. Separate tip/tilt and piston sensing can be used to help uncouple the control system.

2.2 Far-field phase sensing

Far-field phase sensing relies on using a far field image to compute parameters for the control system. This type of sensor is much simpler than a Shack-Hartmann sensor or an interferometer, in that it takes a single measure of the image to compute the required actuator motions, no matter (within limits) how many segments. In some cases this measurement consists of an image captured on a CCD camera, and in others it will consist of a single point measurement. This measurement can be used as a measure of piston, tip or tilt, or the appropriate combination. This leads to considerably less mechanical and optical complication, although at some cost in system performance and software complexity.

The problem with far-field sensing is that it is not possible to uniquely determine the phase of the beam from a single far-field image. The intensity profile will indicate only that the phase is not uniform. Many different realizations of the phase could produce similar images. The phase must be computed from a number of measurements taken successively.

There are several techniques that can be used to compute the actuator positions. In most cases a merit function is computed from the far-field image. This can consist of a single measurement of light that passes through a pinhole, or of a more sophisticated calculation like a radius weighted intensity function, computed from a CCD image, or with a focal plane mask. Some sort of hill climbing algorithm is then applied to improve the image on successive iterations[14, 15]. If the system has relatively slow disturbances then this should be adequate to optimize the phase. Several optimization schemes which do not employ derivatives can be applied. The disadvantage of this scheme is that it requires many iterations to control the phase, and it is never certain that the best solution has been found. We hope to investigate some of these techniques.

Another approach is the neural network approach. A neural net computer can be trained to recognize better images through the use of a merit function or other scheme. The net can then be used to continuously improve the image. This scheme has been applied to phasing the Multi-Mirror Telescope (MMT)[16] with some success.

One problem with using a far-field image for wavefront sensing is that it is limited to a few degrees of freedom. This is because as the number of mirror segments is increased, eventually the effect of changing one degree of freedom causes essentially no change on the resultant far-field image. Lockheed[14] has demonstrated using simplex for phasing up to 19 mirror segments with some success, however, it is doubtful that it can be scaled beyond this point.

One solution to this problem is to use a multi-tiered approach to the wavefront sensing. Figure 1 presents such a scheme. In this case a far-field sensor will look at a few beamlets and close the loop to control these. Since only a few degrees of freedom are being used, this should work well. This control is performed in parallel with several separate far- field wavefront sensors for all of the segments. By creating an overall far-field image, and controlling the segments through offsets applied in groups, the beam can be stitched together. It can be shown that there are advantages to this technique in that it greatly reduces the computational load on the control system. The cost is added complexity of the sensor. Even so, this type of sensor is likely to be considerably simpler than an interferometric phase sensor.

Another possible approach to the wavefront sensing and control problem is to use a hybrid scheme. This is

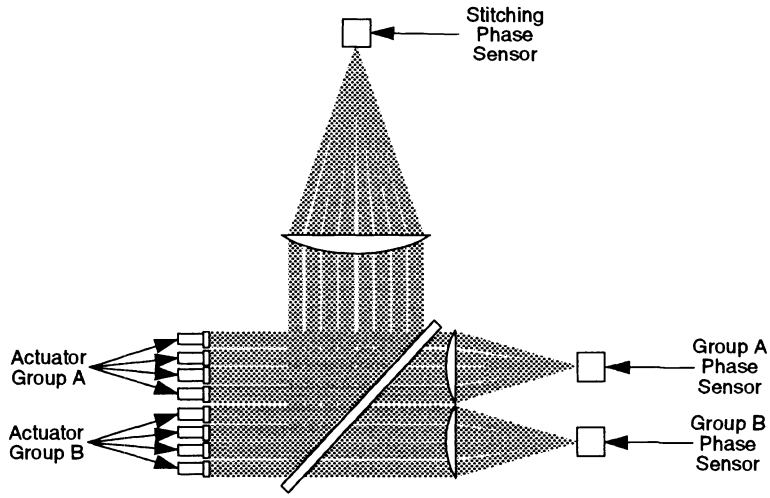

Figure 1: Multi-tiered far-field wavefront sensing and control.

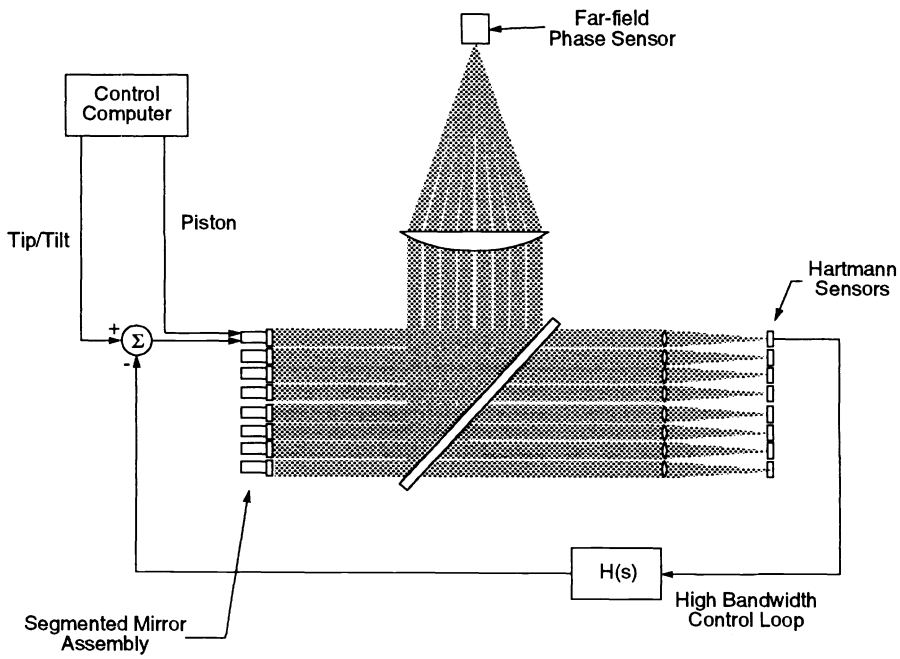

Figure 2: Hybrid Shack-Hartmann/far-field wavefront sensing and control.

presented in Fig. 2. The hybrid scheme uses a Shack-Hartmann sensor to control the tip/tilt of each mirror segment. Since a Shack-Hartmann sensor is relatively simple, and each sensor element controls one mirror segment, the control system is uncoupled. The far-field sensor is used to control only the piston of the resultant beam. This scheme has potential advantages in reducing the number of degrees of freedom needed for the far-field optimization, and maintaining the mirror pointing to high accuracy. If it can be shown that the tip/tilt aberrations for a given laser system occur at higher bandwidth than the piston aberrations, then this may be a natural choice.

One of the major goals of this work is the evaluation of the hybrid and far-field wavefront sensing schemes.

2.3 Interferometer techniques

There are a number of techniques based on interfering beams from adjacent channels[17, 18, 19]. The advantage of these techniques is that, since the phase is measured directly, the control process can be partially decoupled. Two basic approaches have been used. One is the use of a shear plate to measure the relative phase of adjacent beams. This scheme is quite robust and is directly extensible to hundreds of beams[5, 6, 7]. In addition, by controlling the amount of shear added to the beam, the tip and tilt of each beam can be determined uniquely.

The other technique is to use a Shack-Hartmann sensor to control the tip/tilt of the beams, and then interfere small samples from adjacent channels. This has been applied for phasing the output from multiple mirror beam projecting telescopes[20].

Both of these techniques have been demonstrated to work well, although they required a significant amount of specialized data processing in order to calculate the required quantities fast enough. TTC has built a series of specialized computers that are designed to reduce the wavefront sensor data and calculate the control matrices at high bandwidth[7]. Interfering adjacent beams requires the reduction of fringe position data, a process that may be susceptible to noise degradation.

Using the test bed developed for this work, we intend to investigate several of these approaches. This will allow us to investigate the scaling to larger numbers of segments in terms of complexity, cost and performance.

3. SCOPING EXPERIMENT

To begin developing the required hardware and software, and address some of the sensor issues, we developed a scoping experiment that facilitated evaluation of the various techniques, and provide a simple testbed to develop the requirements for the brassboard system. We used only off-the-shelf hardware with lead screw type actuators. These were known to have poor performance for a dynamic environment, but they allowed significant development to proceed during the brassboard design and fabrication.

3.1 Description

Figure 3 shows a schematic of the initial configuration of this experiment. The beam was generated by a small (9mW) Helium-Neon laser and then passed through a six- inch diameter beam expander. The planar wavefront exiting the beam expander was reflected by a pair of two-inch square mirrors, inducing relative tip, tilt, and phase differences between the two beams. These beams were then reflected off of the two active mirrors and onto the wavefront sensor. We will examine these last two components in some detail.

The active mirrors were two-inch square mirrors mounted on a pair of standard tip/tilt stages driven by lead-screw actuators. Each DC motor-driven actuator produced either tip or tilt for one mirror. One of the tip/tilt stages was mounted on a similarly motorized linear stage. Actuation of this motor provided piston movement for one mirror, which was measured by an eddy current sensor. Because of friction and backlash, these devices were very difficult to control to the required resolutions.

The wavefront sensor consisted of a Shack-Hartmann tip/tilt sensor and a phase sensor, which were separated initially to allow us to evaluate some of the far-field and hybrid sensing concepts. The Shack-Hartmann tip/tilt sensor was composed of a pair of lenses that focused each individual beam onto a lateral-effect photodiode to sense the horizontal and vertical position of the focused spot. Phase sensing was accomplished by focusing both beams onto a silicon photodiode. Maximization of the intensity of the focused spot indicated the beams were in phase.

All of the control functions were implemented on a 33MHz 80386 PC. The computer had an 8-input,16-bit A/D converter and a 6-output, 12-bit D/A converter. The signals that were digitized were the four Hartmann signals, the signal from the intensity detector, and the signal from the piston sensor. These signals were sampled at 300 Hz. There were five PID loops closed inside the computer, one around each of the digitized signals except for intensity.

3.2 Results

Figure 4 shows a typical step response of one of the closed loops. The effect of the dry friction can easily be seen as the response "hangs up" after motion begins until the integrator output builds up to push the system to the commanded position. The effect of the deadband in the actuators may be seen in Figure 5 as the response

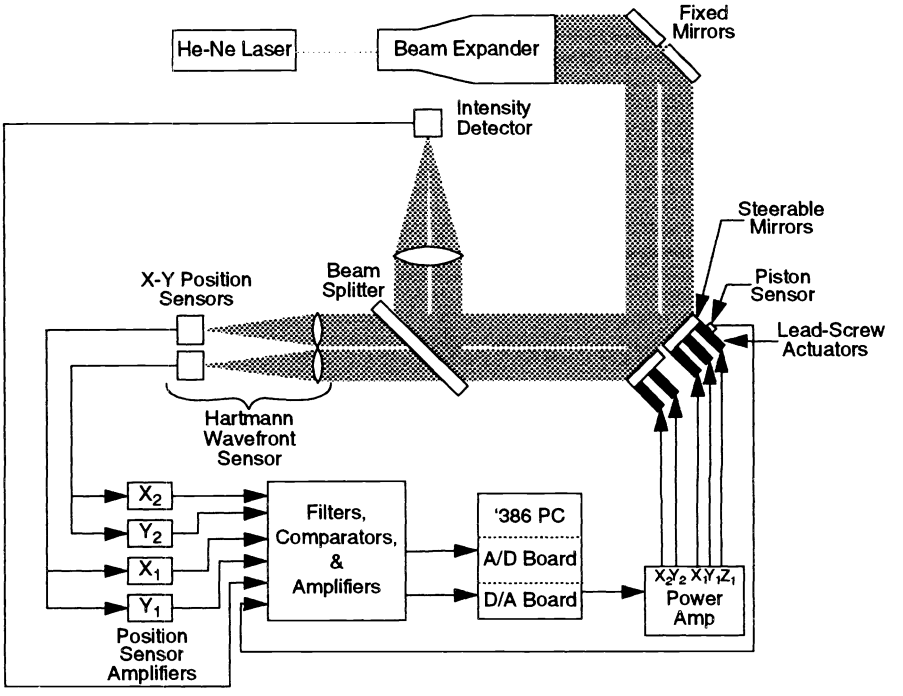

Figure 3: Optical system schematic for the two mirror scoping experiment.

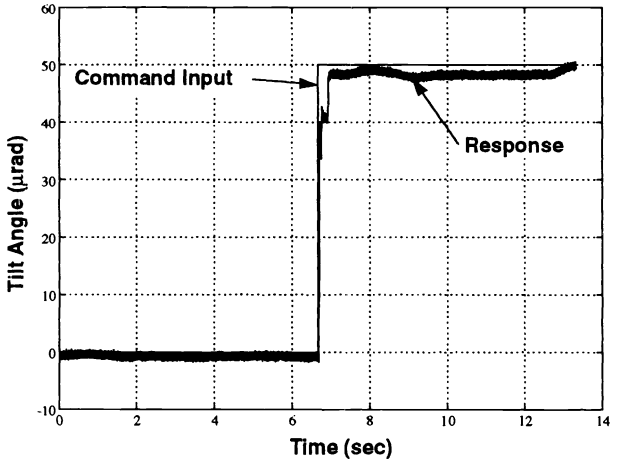

Figure 4: Scoping experiment lead-screw actuator step response.

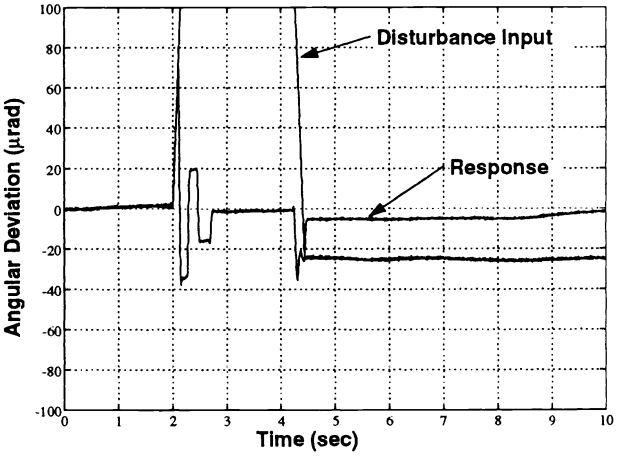

Figure 5: Disturbance rejection for scoping experiment control system.

stops at each point where the direction of the response is changing while the actuators run through their deadband.

The closed-loop bandwidth was difficult to define because of the nonlinearities; but it was very low (< 1 Hz). The signal from the intensity sensor proved useful, as shown in Fig. 6.

The measurements plotted in this figure were single point intensity readings taken at the center of the diffraction pattern of the focused spot. The beams were initially aligned and brought in phase, and then the degree of freedom indicated on the plot was varied for one beam. The shape of the curves is as one would hope, without local maxima to confuse a hill-climbing routine. Tip seems to have a problem in this regard, but the multiple maxima are due to the coupling between tip motion and piston induced by the geometry of the tip/tilt stage. The performance of the actuators was too poor for real-time closed-loop operation of a multiple degree-of-freedom hill-climbing routine, due to the several seconds long settling time. The setup did, however, enable evaluation of far-field wavefront sensing and development of the digital control software. It also helped define the requirements for closed loop control for piston and tip/tilt in order to meet the phasing goal.

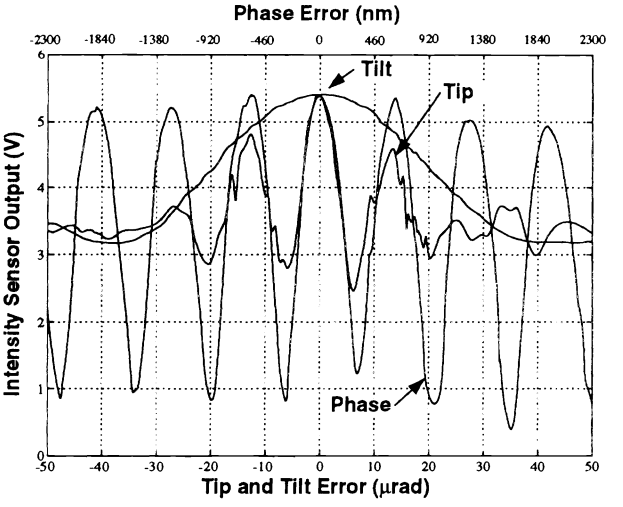

Figure 6: Far-field phase sensor response for tip/tilt and piston disturbances.

4. BRASSBOARD EXPERIMENT

4.1 Description

The next phase of the experiment was to upgrade the mirror actuators. We used commercial Physik Instrumente PZT actuators with strain gauge feedback sensors. The optical setup is essentially similar the the previous experiment, except that the number of channels has been increased and a CCD camera is included for far-field phase sensing. A schematic of the experiment is shown in Fig. 7.

The active mirror configuration is shown in Fig. 8. The four one-inch square, fused silica mirrors are each mounted to a commercially available piezoelectric actuator. As shown in the figure, each actuator is composed of three low-voltage (100V) PZT stacks with strain gages attached. The stacks are preloaded by the housing which includes a flexure. Each stack has a maximum linear travel of 10 micrometers and the assembly has maximum angular travel of 1 milliradian. Because the actuators cannot correct for large static errors due to mounting misalignments, the mirrors must be initially nearly parallel to one another, preferably to within much less than 1 milliradian. They could be mounted and then any misalignment taken out by some mechanical adjustment, but this seems likely to invite mechanical flexibilities and periodic adjustments. Instead, the mirrors were mounted to the actuators using a jig as shown in Fig. 9.

The mirrors were located by a Teflon frame on an optically flat surface and then optically contacted to that surface. The actuators were all rigidly mounted to an Invar base, and three drops of epoxy were placed on the end of each one. An assembly fixture was then used to hold the actuators in the proper orientation with respect to the mirrors while the epoxy set.

A local analog controller drives the difference between the commanded displacement of each piezo stack and its actual displacement (as sensed by the strain gage) to zero. Figure 10 shows a block diagram of the local controller. The closed-loop bandwidth of each actuator is currently about 200 Hz, although this may be improved by further modifications to the local controller, or by bypassing the analog controller altogether and closing the loop inside the digital controller.

The wavefront sensor is similar to the one in the previous experiment. There are Shack-Hartmann sensors that give measurements of the tip and tilt of the four beams. Phase sensing is accomplished by focusing all four beams onto a silicon photodiode. For increased versatility, a CCD camera is being added to obtain an image of the far-field diffraction pattern. The image may be operated on in any one of several ways (e. g., calculating intensity moments) to obtain a merit function to determine the quality of the combined beam. The use of a digital image capturing system should also facilitate

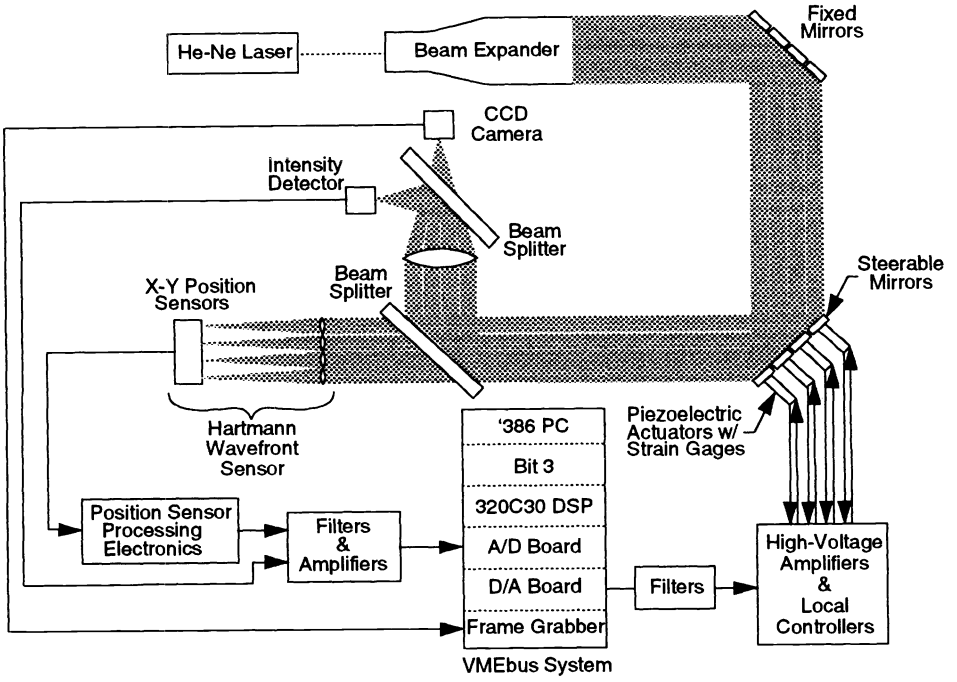

Figure 7: Optical system layout for four-mirror brassboard experiment.

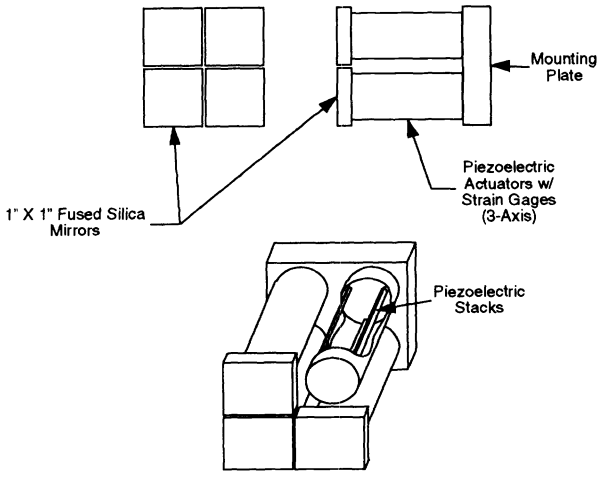

Figure 8: Brassboard experiment actuator/mirror assembly.

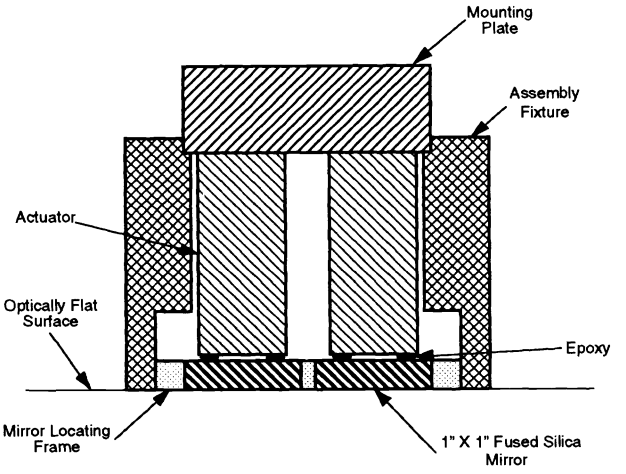

Figure 9: Procedure for assembling mirrors to actuators.

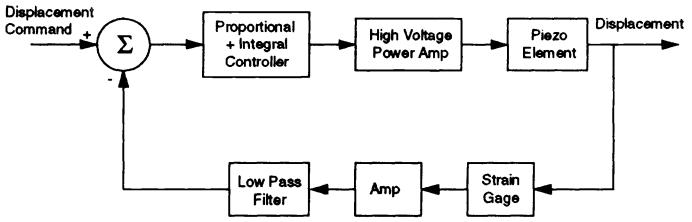

Figure 10: Control diagram for each actuator using strain gauge feedback

the investigation of far- field measurement only, mulit-tiered systems, as far-field images for each tier could be captured on separate areas of the same camera.

The control computer to operate the testbed uses a 386-based PC as a high level host controller for the system. It interfaces to a Texas Instruments TMS320C30-DSP chip which executes at 40 MFLOPS. It has a 16-input, 16-bit A/D and a 16-output, 12-bit D/A. The DSP hardware was chosen to provide a sampling rate that is an order of magnitude greater than the projected bandwidth of the closed-loop system. This will allow full utilization of the capabilities of the piezoelectric actuators. The present configuration also allows easy expandability to accommodate numerous steerable mirrors.

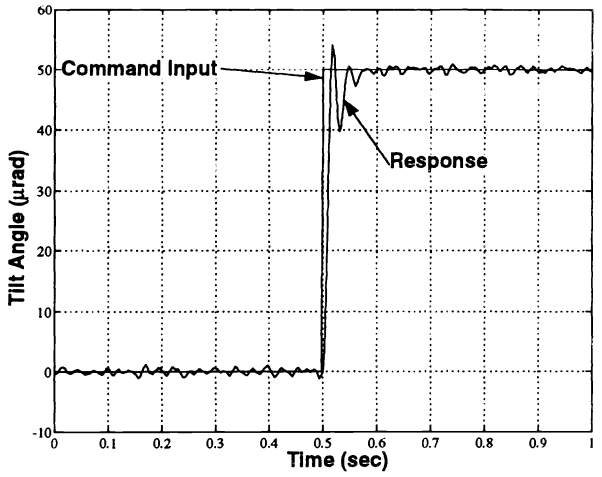

Figure 11: PZT actuator step response.

4.2 Results

The brassboard experiment is still in progress, but some preliminary results are given here. The improvement in actuator performance over the scoping experiment may be seen in the step response shown in Figure 11. The settling time has dropped from several seconds to about 60 milliseconds for this relatively large motion. These data were taken using the '386 PC as the controller. Further improvements will result from incorporating the DSP-based controller.

Figure 12 shows the signal from the photodetector as the relative tilt and phase between the two beams are varied. The change in intensity as piston is varied is more nearly sinusoidal, as is expected. This is due to the greater resolution of the actuators and the proximity of the sensors to the mirrors. Since tip and tilt are generated by combinations of movements of the three PZT stacks, the motions can be calibrated so that there is no coupling between piston and tip/tilt. There was no effort at calibration for the data taken for Figure 12, and

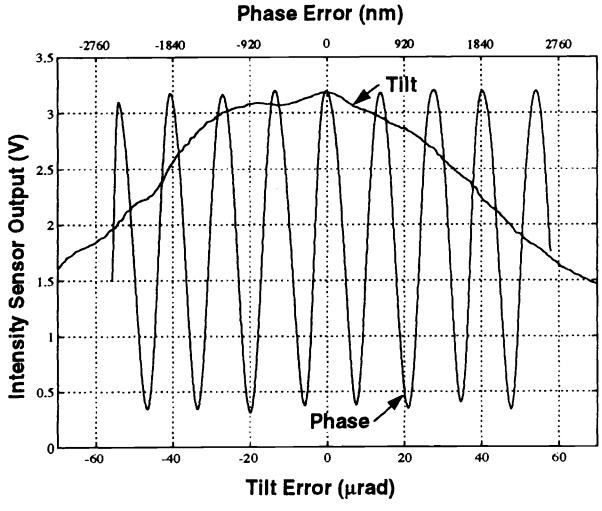

Figure 12: Far-field phase sensor response for phase and tilt perturbations.

the tilt motion appears to be uncoupled to piston.

5. CONTROL ALGORITHMS

The initial control goal was to steer the individual beams from the controlled mirrors to maximize the intensity output from the single photodiode. After these initial experiments, this sensor will be replaced by a CCD camera to improve wavefront sensing. As mentioned before, a byproduct of the sensor output maximization is that the individual, steerable beams would then form a uniform wavefront. Each of the four steerable mirrors has three PZT stacks, whose axes are located 120 deg apart on a circular base for 3-axis control, resulting in 12 total actuating movements.

As an initial foray, it was decided to explore the use of function-evaluation-only parameter optimization programs to do the beam combining. The function-evaluation-only distinction was made due to the fact that our performance metric, either intensity in the case of the photodiode or an intensity weighted merit function measure applied to the output from the CCD camera, is liable to be noisy. This precludes the use of derivative-based optimization schemes, though the number of function evaluations necessary for convergence may be greater. Two schemes of interest are the downhill simplex method[21] and a conjugate-direction search[22].

The downhill simplex was attempted with the original lead-screw actuators. Unfortunately, the settling time necessary for these actuators to attain specified positions to an acceptable tolerance was excessive. Given that an optimization algorithm maps the performance metric to a *unique* parameter space, operation with these actuators did not allow a unique mapping to occur, because the necessary settling time was not attainable. This necessitated the upgrade of the actuators to the PZT stacks.

As implemented here, only two of the mirrors were used for a total of 6 PZT stacks, or parameters for the simplex algorithm. A "function evaluation" consisted of the 6 digital-to-analog (D/A) operations to control the PZT stack lengths plus the single analog-to-digital (A/D) operation to read the photodiode output. An example of the convergence of the simplex scheme for the 6-parameter system is shown in Fig.13. Results for both PZT stack and photocell voltages were normalized against their maximum magnitudes. The photocell output (denoted by the "+" signs) can be seen rising and settling to its maximum value within the noise band of the sensor after 80 iterations. Though this output was noisy, the scheme still tended to converge to the simplex geometry of parameters. Note that the voltages for the PZT stacks in mirror 1 are relatively close together, indicating a predominately piston motion of the mirror, while mirror 2 shows motion about an axis parallel to a line between the y and z stack axes. The fact that in some cases the optimization scheme is adjusting primarily the overall piston of the device is an indication that the hybrid control schemes may have some utility. We hope to address these issues in the next phase of research. The relatively high bandwidth of piezoelectric actuators makes the utilization of these optimization schemes practical. A hardware demonstration of the simplex scheme with PZT stacks was initially done by Mehta et al. at Lockheed in Palo Alto[14].

Since the metric (i.e., photodiode output)is noisy, the parameters tend to converge before the photodiode output, if a typically tight convergence tolerance is used. In addition , the simplex scheme (and other optimization schemes formulated for deterministic applications) have *no* disturbance rejection. In the presence of a disturbance, a method must be built in to alert the process that its "unique" parameter space has changed, and that it needs to either reinitialize itself, or take some other form of action to continue effective beam-combining.

While simplex as described in Ref.[21] does not have the proper characteristics for closed loop control since it continues to look for unique spaces, it gives a good starting point for research in this area. We are currently pursuing several modifications and other optimization schemes that will be used to improve the performance in this area. In addition, we are pursuing the use of neural net control as another alternative.

7. CONCLUSIONS

We have designed and built a four mirror testbed for beam combining multiple lasers. So far the testbed has demonstrated about 30 Hz closed loop response in tip/tilt, and has phased two beams in tip/tilt and piston using optimization. We are currently evaluating several far-field wavefront sensing schemes, including hybrid, multi-tiered and neural net. The four mirror brassboard will be an ideal testbed for evaluating the control schemes scalability to large numbers of beams.

8. ACKNOWLEDGMENTS

The authors would like to acknowledge M. Johnson and T. S. McKechnie for their assistance with the optical setup. This work was performed at Sandia National Laboratories, supported by the U. S. DOE under contract number DE–AC04–76DP00789.

8. REFERENCES

1. L. Sutter, P. Baily, G. Wakalopulos, R. Hill, E. Peressini, F Dolezal, "Holographic interferometry of a

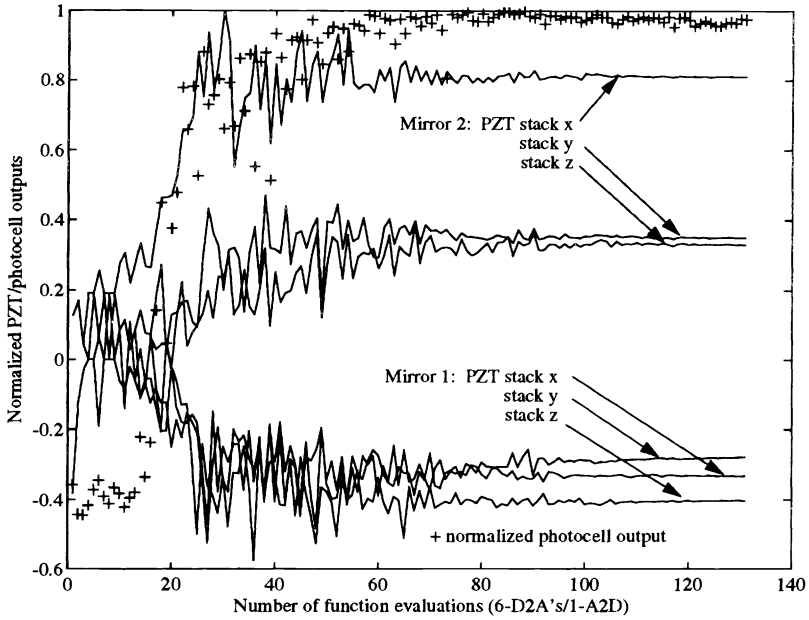

Figure 13: Simplex far-field intensity optimization for two of the four mirrors.

large bore cw high energy gas laser medium during laser power extraction," Appl. Optics Vol. **18**, pp. 3835-3837, 1979.

2. W.P. Latham, M.E. Rogers, and G.E. Palma, "A review of laser device coupling techniques", SPIE Vol. 1224, *Optical Resonators*, pp. 184-201 (1990).

3. R. Fugate,"The current status of the Starfire Optical Range adaptive optics system," SPIE Vol. 1920. *Active and Adaptive Optical Components and Systems II*, (1993).

4. A. Doel, C. Dunlop, J. Major, R. Myers and R. Sharples, "MARTINI: System Operation and Astronomical Performance," SPIE Vol. 1542 *Active and Adaptive Optical Systems*, pp. 319–326 (1991).

5. P. Johnson, R. Tirssel, L.Cuellar, B. Arnold, D. Sandler, "Real time wavefront reconstruction for a 512 subaperture adaptive optical system," SPIE Vol. 1543 *Active and Adaptive Optical Components* pp. 460-471 (1991).

6. B. Hulburd, T. Barrett, L. Cuellar, D. Sandler, "High Bandwidth, long stroke segmented mirror for atmospheric compensation," SPIE Vol. 1543 *Active and Adaptive Optical Components* pp. 64-75 (1991).

7. L.Cuellar, P. Johnson, and D. Sandler, "Performance tests of a 1500 degree-of-freedom adaptive optics system for atmospheric compensation," SPIE Vol. 1542 *Active and Adaptive Optical Systems*, pp. 468–476 (1991).

8. D. Acton and R. Smithson, "Solar imaging with a segmented adaptive mirror," Appl. Optics, Vol. 31, No. 16 pp. 3161–3169,(1 June 1992).

9. D. Acton and R. Smithson, "Solar astronomy with a 19-segment adaptive mirror," SPIE Vol. 1542 *Active and Adaptive Optical Systems*, pp. 159–164 (1991).

10. C. Witthoft, "Wavefront sensor noise reduction and dynamic range expansion by means of optical image intensification," Opt. Eng. **29**(10), 1233–1238 (October 1990).

11. L. Schmutz, "Hartmann sensing at Adaptive Optics Associates," SPIE Vol. 779 *Electromechanical System interaction with Optical Design*, 13–17 (1987).

12. D. D'Amato, S. Barletta, P. Cone, J. Hizny, R. Martinsen, L. Schmutz, "Fabrication and Testing of Monolithic Lenslet Module (MLM) Arrays," Optical Fabrication and Testing Topical Meeting, 1990 Technical Digest Series, Vol. 11, June 12–14, 1990.

13. A. Gleckler, D.J. Markason, G.H. Ames, "PAMELA: control of a segmented mirror via wavefront tilt and segment piston sensing," SPIE Vol. 1543, *Active and Adaptive Optical Components*, pp. 176-189 (1991).

14. N. Mehta and C. Allen, "Remote alignment of segmented mirrors with far-field optimization," Appl. Optics, Vol 31, No.30, pp. 6510-6518 (1992).

15. R. Tyson, "Measuring phase errors of an array of segmented mirror with a single far-field intensity distribution," SPIE Vol. 1542 *Active and Adaptive Optical Systems*, pp. 62–75 (1991).

16. P. Wizinowich, M. Lloyd-Hart, B. McLeod, D. Colucci, R. Dekany, D. Wittman, R. Angel, D. McCarthy, B. Hulburd and D. Sandler, "Neural network adaptive optics for the Multiple Mirror Telescope," SPIE Vol. 1542 *Active and Adaptive Optical Systems*, pp. 148–158 (1991).

17. M Feldman, D. Mockler, R. E. English, J. Byrd, an J T. Salmon, "Self-referencing Mach-Zehnder interferometer as a laser system diagnostic," SPIE Vol. 1542 *Active and Adaptive Optical Systems*, pp. 490–501 (1991).

18. E. Hochberg, "Optical figure testing of prototype mirrors for JPL's Precision segmented reflector (PSR) program," SPIE Vol. 1542 *Active and Adaptive Optical Systems*, pp. 511–522 (1991).

19. N. Nerheim, "A fiber-coupled heterodyne interferometer displacement sensor," SPIE Vol. 1542 *Active and Adaptive Optical Systems*, pp. 523–533 (1991).

20. J.M. Bernard, R.A. Chodzko, and J.G. Coffer, "Master oscillator with power amplifiers: Performance of a two element CW HF phased laser array, Appl. Opt. 28, 4543 (1 Nov 1989).

21. J.A. Nelder, R. Mead, "A Simplex Method for Function Optimization",*Computer Journal*, Vol. 7, p.308 (1965).

22. R.P. Brent, *Algorithms for Minimization without Derivatives*, Prentice-Hall, Chapter 7, 1973